Climate-driven biogenic emissions alleviate the impact of man-made emission reduction on O_3 control in Pearl River Delta region, southern China

Nan WANG[1,2]*, Song LIU[1], Jiawei XU[3], Yanyu WANG[2], Chun LI[1], Yuning Xie[4], Hua LU[5]*, Fumo YANG[1]

[1]College of carbon Neutrality Future Technology, Sichuan University, Chengdu 610065, P. R. China

[2]State Environmental Protection Key Laboratory of Formation and Prevention of Urban Air Pollution Complex, Shanghai Academy of Environment Sciences, Shanghai 200233, P. R. China

[3]Centre for Geography and Environmental Science, University of Exeter, Penryn, United Kingdom

[4]Guangxi Key Laboratory of Emerging Contaminants Monitoring, Early Warning and Environmental Health Risk Assessment, Nanning 530028, Nanning, P. R. China

[5]Chongqing Institute of Meteorological Sciences, Chongqing 401147, P. R. China

***Correspondence:** WANG Nan (nan.wang@scu.edu.cn) and LU Hua (vibgyor0113@163.com)

Key Points

1. Summer O_3 concentrations in the Pearl River Delta region is increasing over the past decade.
2. Climate-driven BVOC emissions take up ~ 80% of the total increasing BVOC emissions from 2001 to 2020.
3. The rising BVOC emissions serve as a key factor in the unexpected rise of O_3 levels.

Abstract

O_3 concentrations in the Pearl River Delta (PRD) during summer are typically low and often overlooked. However, integrated observational data reveal a consistent increase in summer O_3 levels over recent decades (+0.96 ppb/year), contradicting China's efforts to reduce anthropogenic emissions. Our dynamically calculated natural emissions show that biogenic volatile organic compound (BVOC) emissions in the region significantly increased between 2001 and 2020, primarily due to climate change and alterations in vegetation cover, with climate-driven BVOC emissions accounting for approximately 80% of the increase. Furthermore, parallel simulations using the WRF-CMAQ model indicate that climate-driven BVOC emissions, by enhancing atmospheric oxidative capacity and accelerating O_3 formation, have weakened or even offset the benefits of anthropogenic emission reductions, contributing 6.2 ppb to O_3 formation and leading to an unexpected rise in O_3 levels. This study enhances our understanding of the mechanisms behind natural emissions in urban O_3 formation under climate change and provides insights for future O_3 pollution control strategies.

Key words: BVOC emission, O_3 pollution, climate impact

Plain Language Summary

This study examines the rising levels of ozone (O_3) pollution in the Pearl River Delta (PRD) region during summer, a time when O_3 concentrations are typically low. Despite efforts by China to reduce pollution from human activities, our research shows that O_3 levels have consistently increased over the past few decades. We found that emissions of biogenic volatile organic compounds (BVOC) from plants have significantly risen from 2001 to 2020, mainly due to climate change and changes in vegetation. Notably, about 80% of this increase in BVOC emissions is driven by climate factors. Our simulations suggest that these climate-driven BVOC emissions are counteracting the benefits of efforts to reduce human-made emissions, contributing significantly to O_3 formation. This research helps us understand how natural emissions influence urban O_3 levels, particularly under changing climate conditions, and provides valuable insights for future pollution control strategies.

Introduction

Tropospheric ozone (O_3) is formed through photochemical reactions involving its precursors, volatile organic compounds (VOCs), carbon monoxide (CO) and nitrogen oxides (NOx), under ultraviolet light. High concentrations of tropospheric O_3 not only pose a threat to human health but also harm agricultural crops and other aspects of the ecosystem (Lippmann, 1989; West et al., 2006; Xiao et al., 2021; Feng et al., 2022). Despite the strict emission reduction measures implemented since the so called "National Ten Measures" (Air Pollution Prevention and Control Action Plan, 2012-2017) and the "Blue Sky Protection Campaign" (2017-2020) in China, O_3 pollution has been rapidly increasing and spreading across larger areas, becoming the primary pollutant in many regions of China (Wang et al., 2017; Lu et al., 2018; Wang et al., 2019; Lyu et al., 2023).

Current research on O_3 pollution in China primarily focuses on anthropogenic emissions, with limited attention given to natural sources, such as biogenic volatile organic compounds (BVOCs). BVOCs are highly reactive and, once released, rapidly interact with atmospheric oxidants such as hydroxyl radicals (OH), leading to increased concentrations of O_3 and other oxidative products. (Jenkin and Clemitshaw, 2000; Fry et al., 2014; Cao et al., 2022; Gao et al., 2022; Wang et al., 2022b). In urban environments with high nitrogen oxide levels, O_3 formation is particularly sensitive to VOCs, meaning that even low concentrations of BVOCs can significantly impact O_3 levels. For instance, BVOC emissions from urban greening spaces, in combination with anthropogenic emissions, can contribute to an additional increase of approximately 5 ppb in O_3 concentrations in Beijing(Ma et al., 2019). Likewise, the intermediate oxidation products of BVOCs, such as methyl vinyl ketone (MVK) and methacrolein (MAC) from South China's forests, can interact with anthropogenic emissions from the Yangtze River Delta (YRD) and Pearl River Delta (PRD) urban clusters through regional transport, leading to elevated O_3 levels in downstream cities(Wang et al., 2022b).

It is important that the BVOC emissions, particularly isoprene emissions, are closely

related to meteorological conditions. Typically, isoprene emissions increase with rising temperatures (or solar radiation); however, when temperatures become too high, vegetation growth is inhibited, and isoprene emissions may decrease due to stomata close (Seco et al., 2022). Recent research has found that under mild to moderate heat stress, reduced stomatal conductance in vegetation leads to increased leaf temperatures, which can indirectly enhance isoprene emissions from plants (Wang et al., 2022a). Numerous studies have found that synoptic weather systems with high temperatures significantly exacerbate BVOC emissions from vegetation. For instance, several studies have report that the rare heatwave during the summer of 2022 exacerbated O_3 pollution by intensifying BVOC emissions in the YRD, PRD and Sichuan Basin regions (Li et al., 2024; Wang et al., 2024b; Wang et al., 2024a).

The Pearl River Delta (PRD) is a typical developed urban cluster located in southern China. This region is characterized by distinct geographical features: urban areas are characterized by high levels of anthropogenic emissions, while the surrounding areas are densely vegetated. Due to climate change and ongoing greening efforts, vegetation in this region has significantly increased, particularly the evergreen broadleaf forests, which are known for their high BVOC emissions. (Guenther et al., 2006; Guenther et al., 2012; Wang et al., 2023a). Currently, air quality issues in the PRD have shifted from $PM_{2.5}$-dominated haze pollution to O_3-dominated photochemical pollution. A substantial amount of research has been conducted on the characteristics of O_3 pollution. For example, Yin et al. (2019) found that summer O_3 concentrations in the region are relatively low due to monsoon influence, with higher values observed in autumn; Jin and Holloway (2015) discovered seasonal variations in the sensitivity of O_3 to its precursors, indicating that the cold season is VOCs-limited, while summer often exhibits a NO_x-limited or synergistic control regime. However, past studies have primarily focused on the impact of anthropogenic emissions, with limited attention given to the effects of natural sources. The impact of increased natural emissions from vegetation and climate warming on local O_3 levels remains unclear.

In this study, we combined comprehensive observations to analyze the summer O_3 and

vegetation trends in the PRD region. Using a dynamic MEGAN model for biogenic emissions, we quantified the changes in BVOC emissions caused by vegetation and climate change, and the meteorological factors driving these BVOC changes were also identified. Finally, we would assess the impact of BVOC variations and anthropogenic emission reductions on O_3 levels. This study aims to provide scientific insights into the mechanisms of O_3 pollution and emphasize the importance of control strategies that account for the synergistic effects of both anthropogenic and natural emissions in the context of climate warming.

2.Material and Methods

2.1 Data

We integrated surface O_3 observations with O_3 sounding data to investigate the spatiotemporal variations of O_3 in the Pearl River Delta (PRD) region. The surface O_3 data were sourced from the monitoring network established by China's Ministry of Ecology and Environment (MEE), comprising 89 operational stations across the PRD (Fig. 1). These networks provide in-situ observations of ambient hourly O_3, CO, SO_2, NO_2, $PM_{2.5}$ and PM_{10} concentrations after 2013. In addition, complementary O_3 sounding data were sampled at King's Park, Hong Kong (114.17° N, 22.31° E), where operational O_3 sounding has been conducted since 1993. Soundings are performed weekly at 14:00 local time using balloons, providing vertical profiles with a resolution of approximately 10 m, reaching altitudes of up to ~30 km. In this study, we collected O_3 soundings from the surface up to 900 hPa (within the boundary layer) to represent the background O_3 levels in the PRD region.

In order to understand the nitrogen oxides (NOx), a precursor of O_3, satellite observations and emission inventory were analyzed. Monthly tropospheric NOx column data (Level 3) were obtained from the OMI satellite instrument (data accessed via: https://avdc.gsfc.nasa.gov/pub/data/satellite/Aura/OMI, last access Aug 20, 2024). Anthropogenic NOx emissions were derived from the Multi-resolution Emission Inventory for China (MEIC) developed by Tsinghua University (https://meicmodel.org.cn/, last access Aug 20, 2024).

2.2 MEGAN model

Biogenic emissions were computed offline using the Model of Emissions of Gases and Aerosols from Nature version 2.1 (MEGAN) developed by Guenther et al. (2012). MEGAN model is capable of estimating the emissions of over a hundred biogenic volatile organic compounds (BVOCs), with a horizontal resolution that can range from ~ 500 meters to hundreds of kilometers. The theoretical calculations are based on the following concept:

$$F_i=\gamma_i \sum \varepsilon_{i,j}\chi_j \quad (1)$$

where F_i, $\varepsilon_{i,j}$ and χ_j are emission amount, standard emission factor and fractional coverage of each plant functional type (PFT) j of chemical species i. γ_i is the emission activity factor, which is calculated based on canopy environment coefficient (C_{CE}), leaf area index (LAI), light (γ_L), temperature (γ_T), leaf age (γ_{LAI}), soil moisture (γ_{SM}), and CO_2 uptake (γ_{CI}):

$$\gamma_i = C_{CE}LAI\gamma_{L,i}\gamma_{T,i}\gamma_{LA,i}\gamma_{SM,i}\gamma_{CI,i} \quad (2)$$

In China, most researchers using MEGAN rely on the model's default surface data. However, this default data is based on conditions from the year 2000, with no annual variation. Considering the significant changes in land cover due to China's reforestation policies and climate change, the outdated land surface data fails to capture current conditions accurately. Therefore, this study employs satellite-derived, high-resolution land data with monthly dynamic updates to achieve more representative and accurate estimates of BVOC emissions. In detail, the LAI data are sourced from the MODIS MCD15A2H product covering the period from 2001 to 2020, with a temporal resolution of 8 days. The land cover type data are derived from the MODIS MCD12Q1 product, which uses an LAI-based classification scheme and includes 8 vegetation types. These were further mapped to the 16 plant functional types (PFTs) used in MEGANv2.1 with the consideration of the methodology outlined by Bonan et al. (2002) The detailed mapping scheme were provided in the supplementary (Table S1). Meteorological conditions were provided by Weather Research and Forecasting (WRF) simulations.

Using this method, we were capable to separately quantify the impact of vegetation

emissions driven by changes in vegetation distribution and those driven by climate change. For instance, by fixing the meteorological conditions while allowing the vegetation data to change annually, we could isolate the contribution of vegetation distribution variations to emissions (land impact). Similarly, by holding the vegetation data constant and allowing meteorological conditions to vary year by year, the emissions attributable to climate change could be quantified (climate impact).

2.3 Random Forest model

To investigate the relationship between BVOC emissions and meteorological factors, we employed a Random Forest (RF) machine learning model. Since BVOC emissions were calculated based on the MEGAN-calculation framework, where emissions are driven by inputs such as temperature, humidity, solar radiation and etc. This context makes the RF model particularly suitable, as it is adept at handling non-linear relationships and interactions among variables, making it effective for complex environmental datasets. We trained the RF model using the WRF simulated meteorological variables alongside corresponding BVOC emission. To interpret the results and gain insights into the contribution of each meteorological factor to BVOC emissions, we utilized Shapley Additive Explanations (SHAP) values. SHAP values provide a robust framework for understanding the impact of individual features on model predictions by attributing the contribution of each factor to the overall output. This approach not only enhances the interpretability of the RF model but also facilitates a deeper understanding of how different meteorological conditions influence BVOC emissions, thereby informing future research and environmental management strategies.

2.4 WRF-CMAQ model

We employed the WRF-CMAQ (Weather Research and Forecasting-Community Multiscale Air Quality) chemical transport model to assess the effects of climate and land-change-induced BVOC emissions, alongside anthropogenic emission reductions, on O_3 concentrations. The WRF mode (version 3.9.1) is a mesoscale numerical weather prediction system designed for both operational forecasting and atmospheric research. Atmospheric chemistry was simulated using CMAQ (version 5.3), with the Carbon

Bond version 06 (CB06) and Aerosol Module version 6 (AERO6) mechanism. In this study, we utilized a single domain with a horizontal resolution of 25 km, covering the entirety of China and its surrounding regions, centered at 30°N, 106.8°E. The model includes 31 vertical layers with a top pressure boundary of 100 hPa. The WRF model was driven by ERA5 reanalysis data, providing meteorological inputs for the simulation. The chemical boundary conditions for the CMAQ domain were sourced from the Community Earth System Model (CESM).

The key WRF-CMAQ configurations include the Rapid Radiative Transfer Model (RRTM) for longwave and shortwave radiation, the Noah Land Surface Model for land-atmosphere interactions, the Kain-Fritsch scheme for cumulus parameterization, the Lin microphysics scheme, and the YSU boundary layer scheme. Anthropogenic emissions for China were obtained from the Multi-resolution Emission Inventory for China (MEIC), and biogenic emissions were calculated by the improved MEGAN model (described in Section 2.2). The performance of the model was validated by comparing with observations. Generally, the statistical comparisons showed that the model simulated results matched well with those observed, indicating a reliable model performance (summarized in Table S2).

Using the WRF-CMAQ model, we conducted parallel comparison experiments to address the importance of BVOCs emissions. For example, scenarios that consider only anthropogenic emissions (AVOC_Only) versus those that include both anthropogenic and vegetation emissions (Add_BVOC). To explore the complex nonlinear relationships between O_3 and its precursors, we employed the HDDM (High-order Decoupled Direct Method) approach. In HDDM, sensitivity coefficients (S_j) represent the response of a chemical concentration to perturbations in a sensitivity parameter, such as emissions, initial conditions, boundary conditions, or reaction rates (Simon et al., 2013; Itahashi et al., 2015). The semi normalized first- and second-order sensitivity coefficients, $S_j^{(1)}$ and $S_{j,k}^{(2)}$ are defined as follows,

$$S_j^{(1)} = \frac{\partial C}{\partial E_j} \quad (3)$$

$$S_{j,k}^{(2)} = \frac{\partial^2 C}{\partial E_j \, \partial E_k} \quad (4)$$

,where $S_j^{(1)}$represents the first-order sensitivity to changes in parameter *j*. $S_{j,k}^{(2)}$refers to the second-order sensitivity to simultaneous changes in parameter *j* and *k*. When *j*=*k*, $S_{j,j}^{(2)}$means the sensitivity to an individual parameter, and when *j*≠*k*, it refers to a cross-sensitivity coefficient. The equation for approximating O_3 concentrations under the perturbations of parameters j and k through a Taylor-series expansion of the sensitivity coefficients is as follows:

$$C_{(\triangle E_j, \triangle E_k)} = C_0 + S_j^{(1)} \triangle E_j + \frac{1}{2} S_j^{(2)} \triangle E_j^2 + S_k^{(1)} \triangle E_k + \frac{1}{2} S_k^{(2)} \triangle E_k^2 + \triangle E_j \triangle E_k S_{j,k}^{(2)} \quad (5)$$

, where C_0 refers to the chemical concentration in the base scenario.

Besides, O_3 formation budget based on the perspectives of anthropogenic emission reductions and changes in vegetation emissions were quantified over the last decades (2001-2020). This algorithm maximally accounts for the influences of anthropogenic and biogenic sources to highlight their respective contributions in a climatic scale. For instance, anthropogenic NO_x emissions peaked in 2012 and have continuously declined over the past decade. Therefore, we assessed the impact of human emission reductions by comparing O_3 simulations driven by emissions from 2012 and 2020. Similarly, considering the continuous increase in surface vegetation data, we utilized surface vegetation data from 2001 and 2020 to drive the vegetation emissions aiming to maximize the differences in O_3 simulations resulting from changes in vegetation. To account for the impact of climate change-driven vegetation emissions, we calculated BVOC emissions using both current and historical meteorological data. We then examined the differences in O_3 simulations driven by current and past meteorological data. The impact of climate-driven meteorology on chemical O_3 formation could also be identified using similar methods (see details in Table S3). Although this algorithm does not operate within a unified time frame, it emphasizes the contributions of both anthropogenic and vegetation emissions, aiding in the assessment of their combined effects.

3 Results

3.1 Rising summer O_3 concentrations and vegetation in PRD

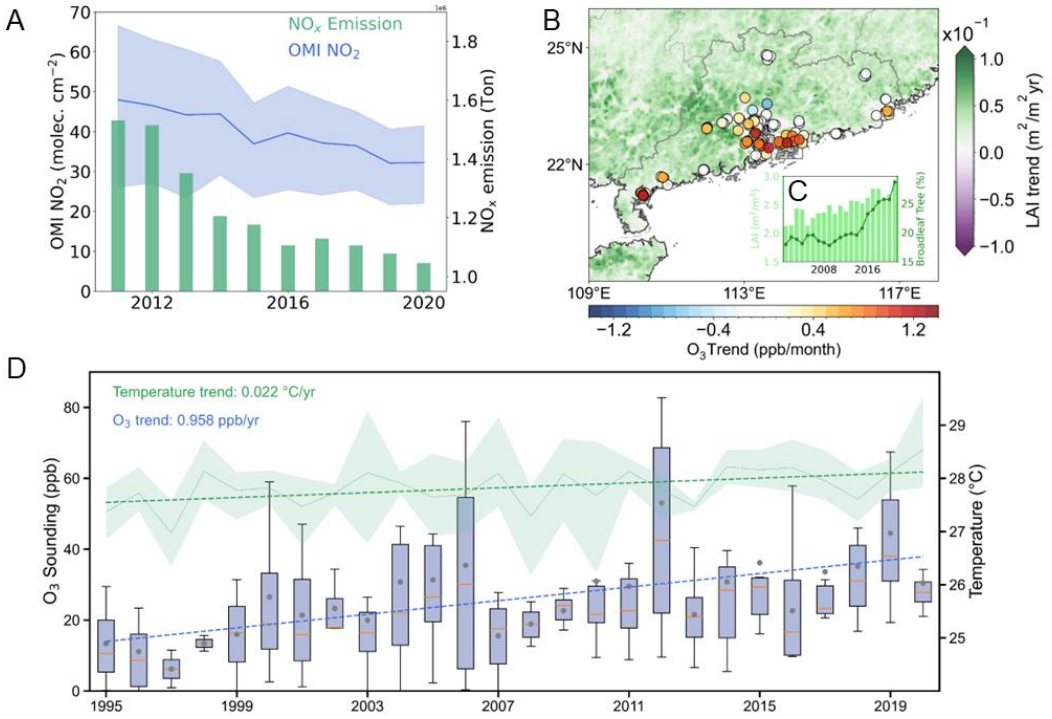

Figure 1 (A) Changes of tropospheric NO_2 column concentrations and anthropogenic NO_x emissions in PRD from 2011 to 2020. (B) PRD map showing surface observed summer O_3 trends (2013-2020) and leaf area index trends (LAI, 2001-2020). (C) Changes of LAI and proportion of broad leaf trees in PRD between 2001 and 2020. (D) Variation of summer O_3 soundings and temperature, the dashed lines were the linear plot.

Since China implemented the "National Ten Measures" in 2012, aimed at controlling $PM_{2.5}$ pollution, NO_x emissions have shown significant improvement in PRD, as evidenced by the substantial annual decline in NO_x column density and emissions from 2011 to 2020 (Fig. 1A). However, surface monitoring summer O_3 concentrations in the PRD region exhibited an upward trend with an increasing rate of 0.51 ppb/month (Fig. 1B). We also examined background O_3 sounding data within the boundary layer (between surface and 900hPa), the results revealed an increasing rate of 0.96 ppb/year between 1995 and 2020, consistent with the surface network observation (Fig. 1C). It has been widely acknowledged that summer O_3 levels in the PRD are generally low due to the monsoon-prevailing southerly winds, which brings relatively clean air from South China Sea. However, the rising O_3 concentrations in recent summers suggest that photochemical O_3 pollution is becoming increasingly severe in the PRD.

Driven by the government's reforestation policies and the impact of climate change, we also observed an increasing trend in vegetation coverage in the PRD, as indicated by the broad positive LAI trend over the last two decades (Fig. 1B). Additionally, through the analysis of changes in vegetation types, it was found a significant increase in the proportion of evergreen broadleaf forests, a tree type known for high BVOC emissions, rising from 17.9% to 28.6% between 2010 and 2020 in PRD (Fig. 1D). The increase of the vegetation coverage implies a potential rise in BVOC emissions, which appears to be a possible contributor to the observed O_3 increment. Additionally, against the backdrop of global climate warming, the PRD has experienced a temperature increase of +0.02°C/year over the past decade (Fig. 1C), which would further enhance BVOC emissions due to elevated temperatures.

3.2 Significant BVOC emission increment due to climate change

Table 1 Comparisons of Isoprene emissions and their proportion of total BVOCs.

Isoprene emission (Tg)	Isoprene/BVOCs (%)	Reference
17.5	53.9	This study
15.94	46.5	Wang et al. (2021a)
9.6	50	Cao et al. (2018)
9.59	50.9	Fu and Liao (2012)
13.3	56.5	Wu et al. (2020)
15	52.8	Guenther et al. (1995)
19.13-27.09	52.4	Li and Xie (2014)
20.7	42.5	Li et al. (2013)
28.23-37.45	57.6-63.6	Li et al. (2020)

As detailed in the methods section, we updated the MEGAN model by incorporating dynamically varying satellite-derived vegetation data. To assess the model's reliability, we calculated the BVOC emissions for the entire year of 2020 in China, utilizing 2020-based meteorology and land data, and compared the findings with results from previously published studies (Table 1). The BVOC inventory established in this study

indicates that total isoprene emissions in China reached 17.5 Tg, falling within mid-range estimates from previous studies (Table 1), suggesting overall consistency with earlier findings. Notably, isoprene accounts for 53.9% of all BVOC emissions, a proportion that also aligns well with earlier findings. This not only supports the validity of our calculations but also underscores the significance of isoprene across all BVOC species.

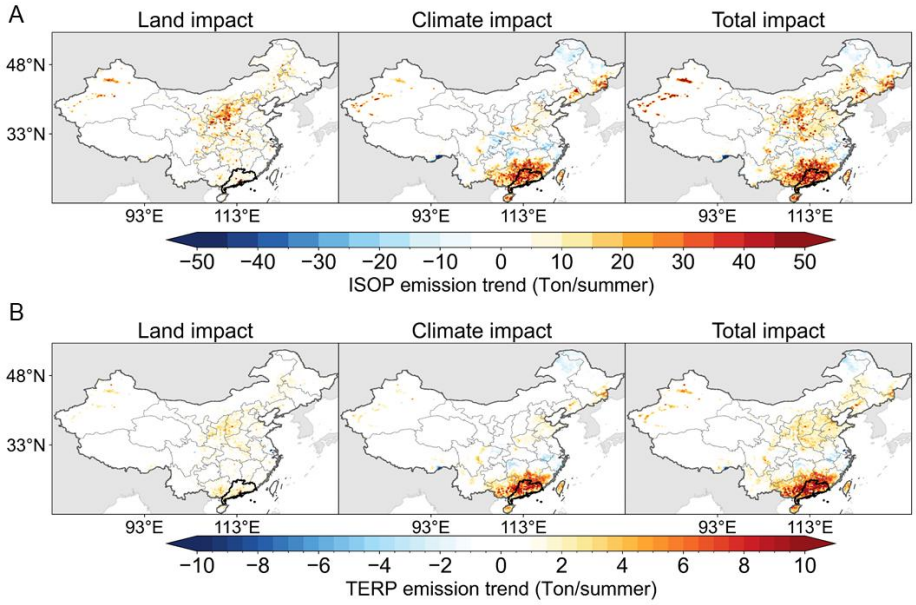

Figure 2. Summer isoprene (A) and terpene (B) emission trend in mainland China between 2001 and 2020. The land impact refers to BVOCs emissions (ISOP for isoprene, TERP for terpene) from vegetation cover change, while the climate impact refers to BVOCs emissions due to climate change. The black line in the map highlights the administrate boundary of the PRD region.

By using different combinations of meteorological conditions and land cover data (including LAI and PFT), we employed the MEGAN model to quantify the impact of land use and climate changes on BVOC emission trends from 2001 to 2020, respectively. The two major components of BVOCs, isoprene and terpenes, were both quantified in response to changes in vegetation cover and climate. Our findings indicate a significant upward trend in both isoprene and terpene emissions in southern China (including PRD) and northern China, which stand in stark spatial contrast to the emissions patterns observed in western and central China. By attributing the emission changes to vegetation and climate shifts, we found that, unlike northern regions of China, such as the Loess Plateau, where increased BVOC emissions are primarily

attributed to afforestation efforts (Zhang et al., 2016), the rise in BVOC emissions in southern China is mainly influenced by climate change. For example, the isoprene emission trend was 30.0 Ton/summer over 2001-2020 in PRD, taking up ~ 80% total isoprene variations. The significant increase attributed to climate change suggests that BVOC emissions in this area are highly sensitive to climatic variations.

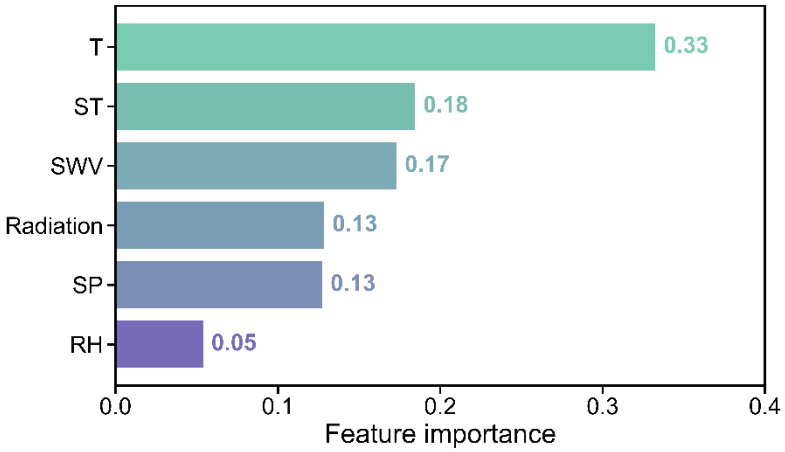

Figure 3. Feature importance of meteorological parameter on BVOCs emissions

The climate impact could be simply attributed to the combined effects of multiple meteorological parameters, such as ambient temperature, soil temperature, relatively humidity and so on. It is crucial to identify the dominant meteorological factors under the context of climate warming. To this end, we established a diagnostic method that coupled numerical model with machine learning. Specifically, we utilized meteorological parameters simulated by the WRF model to drive a Random Forest (RF) model aimed at training BVOCs emissions. To ensure the robustness of the results, we performed a 10-fold cross-validation, achieving an R^2 (coefficient of determination) of 0.78 and an MAE (mean absolute error) of 0.73, respectively (Fig. S1). These metrics indicate that the machine learning model effectively reproduces BVOC emissions. To assess the significance of each meteorological parameter, we employed the SHAP (SHapley Additive exPlanations) method (see details in methods). The results indicated that ambient temperature, soil temperature, soil water vapor, radiation, surface pressure, and relative humidity are the dominant meteorological parameters, with temperature being the most influential. This finding is further supported by the observed upward

trend in these parameters over the past 20 years (Fig. S2). Our investigation reveals that BVOC emissions in PRD are highly sensitive to the climate and the rising temperature has become the dominant factor driving the increase in BVOC emissions. Noting that the PRD is a developed city clusters with high anthropogenic emissions, the annual rise in BVOC emissions is likely to exacerbate the interactions between natural and human-made emissions. Therefore, the impact of BVOCs emissions warrants further exploration in addressing the issue of increasing summer O_3 levels in the region.

3.3 Climate induced BVOC alleviates O_3 control

To quantify the influence of BVOC on O_3 concentrations, the CMAQ-HDDM model was employed to assess the sensitivity of O_3 to its precursors during the summer of 2020 in southern China. The response of atmospheric oxidation capacity to BVOC emissions was evaluated under two scenarios: one considering only the impact of anthropogenic VOCs (AVOC_ONLY scenario), and the other accounting for both anthropogenic and biogenic emissions (ADD_BVOC scenario). Noting that the AVOC_ONLY scenario is an unrealistic scenario and removing BVOCs emissions from the real-world may result in uncertainties due to the non-linear relationship between O_3 and its precursors, however, studying and comparing the parallel numerical experiments (AVOC_ONLY and ADD_BVOC scenarios) could greatly help us understand the mechanisms and significance of BVOC emissions on O_3 formation. In each scenario, we primarily focused on the responses of O_3 to NO_x emission reductions, aligning with China's emission control strategy that predominantly targets NO_x emissions.

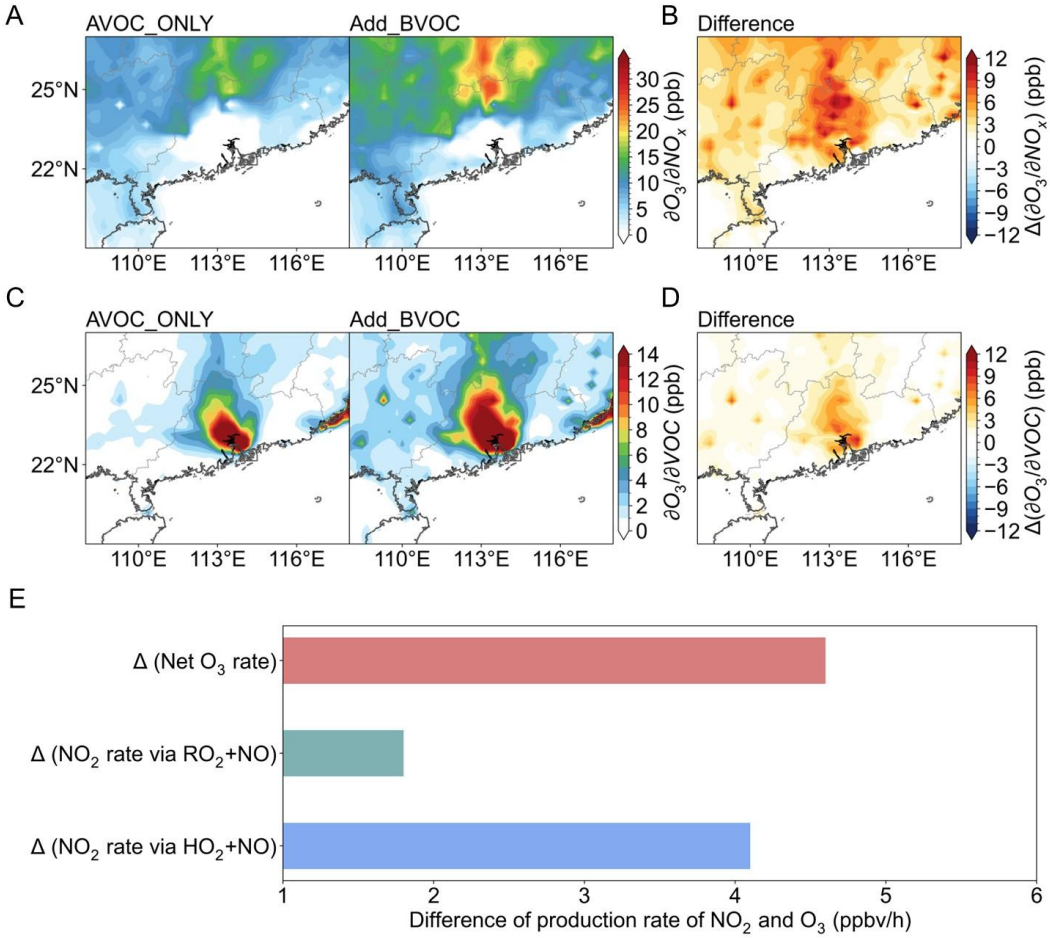

Figure 4. (A) Spatial distribution of O_3 sensitivity coefficients to NO_x emissions under AVOC_ONLY and Add_BVOC scenario. (B) Difference of O_3 sensitivity coefficients to NO_x emissions between Add_BVOC and AVOC_ONLY scenario. (C) Same as (A) but for sensitivity coefficients to VOCs emissions. (D) Same as (B) but for O_3 sensitivity coefficients to VOCs emissions (E) difference of production rate of NO_2 (via chemical pathway of RO_2+NO and HO_2+NO) and net production rate of O_3 at 14:00 between Add_BVOC and AVOC_ONLY scenario

Taking the 2020-based simulation as an example, we analyzed the spatial distribution of the first-order sensitivity coefficient of O_3 to its precursors (Fig. 4). Under the AVOC_ONLY scenario, the central region of the PRD exhibited significant sensitivity to VOC emissions (i.e., high sensitivity coefficients were over 15 ppb), while the surrounding areas were more NOx-sensitive (Fig. 4A and 4C). When BVOC emissions were included, the VOC-sensitive region expanded beyond the core of the PRD to its surrounding areas, also with an increase in the sensitivity coefficient value. This implied that a more favorable condition for O_3 production. Additionally, in remote areas that belonged to NO_x-sensitive, for instance the northern PRD, a notable increase of the sensitivity coefficient value was found, meaning the sensitivity of O_3 to NO_x emissions

also became more pronounced (Fig. 4B and 4D). This suggests that even in NO_x-limited regions, BVOCs could significantly enhance atmospheric reactivity, facilitating easier O_3 formation. The underlying mechanism by which BVOC emissions influence ozone formation can be attributed to their impact on NO_2 production levels (Fig. 4E). By comparing the reaction rates of RO_2 + NO and HO_2 + NO, both key pathways determining O_3 formation, we found that the addition of BVOCs increased these reaction rates by 4.1 ppb/h and 1.8 ppb/h, respectively. In other words, the presence of BVOCs enhanced atmospheric oxidizing capacity, leading to an additional O_3 production rate of approximately 4.7 ppb/h. Further, we simulated O_3 responses to NO_x emission perturbations under both scenarios (Fig. S3). The result showed that O_3 levels initially rose and then fall as NO_x reductions increased, with a turning point around a 10% emission reduction. Compared to our previous study conducted in winter, which identified the O_3 formation regime as transition-limited with a turning point at approximately 35% NO_x emission reduction (Wang et al., 2021b), it is believed that O_3 formation sensitivity in the PRD during summer is more closely aligned with a NOx-limited regime. However, after considering the influence of BVOC emissions, the benefits of NOx reduction were offset by the influence of BVOC emissions, which contributed an additional ~ 5 ppb of O_3 formation.

Next, leveraging scenario simulations with the CMAQ model, we quantified the O_3 formation budget from the perspectives of anthropogenic emission reductions and changes in vegetation emissions over the past decades (Fig. 5). Despite the implementation of China's "Ten Measures" (2012-2017) and the "Blue Sky Protection Campaign" (2017-2020) pollution control strategies, observational data have shown a rise in O_3 levels, which contradicts expectations and has puzzled policymakers in formulating effective O_3 control strategies. These contrasting effects largely stem from shifts in O_3-NO_x-VOCs sensitivity. Past studies suggested that O_3 levels would temporarily increase in the short term following NO_x emission controls (Wang et al., 2019; Huang et al., 2021). However, after a long-term (nearly a decade) emission reductions, our finding reveals that, when considering only anthropogenic emissions

(AVOC_ONLY scenario), emission reductions could lead to varying degrees of O_3 decline in southern China. For example, the average O_3 concentrations in Guangzhou could potentially decrease by 9.8 ppb due to man-made emission control (Fig. 5A). This result was consistent with a recent study by Wang et al. (2023b). However, the "benefit" has been overshadowed by the increase in BVOC emissions (ADD_BVOC scenario). Our research indicated that the key driver of rising summer O_3 levels was the significant impact of BVOC emissions. Specifically, BVOC emissions driven by climate warming significantly impacted O_3 concentrations, showing a pronounced positive effect in the core of the PRD urban areas (Fig. 5B). In Guangzhou, climate-driven BVOC emissions have contributed to an increase in O_3 levels by as much as 6.2 ppb. In comparison, BVOC emissions resulting from vegetation distribution variations (vegetation-change BVOC) contributed less to O_3 formation, but still had a positive impact, with a contribution ranging from 0.8 to 1.5 ppb. It is noteworthy that the contribution of climate impact on O_3 chemistry (Climate-driven chemistry) varied significantly, with values ranging from -19.3 to 16.2 ppb. This substantial difference might be attributed to perturbations caused by extreme weather events. For instance, extreme stable weather conditions, such as heatwaves, are conducive to O_3 pollution, while intense heavy rainfall facilitates O_3 removal. ~~Indeed, the PRD is highly susceptible to extreme weather events during the summer, such as the periphery of typhoons (heatwaves) and strong rainfall brought by squall lines.~~ By analyzing historical monthly average temperature and precipitation in the PRD from 2000 to 2020, we found that both summer temperature and precipitation exceed the climatic monthly average, ranking the highest among the four seasons (Fig. S4). This result aligns with our description, on one hand, hot days (i.e., the periphery of typhoons, and heatwaves) enhance photochemical O_3 formation, while on the other, extreme precipitation (i.e., squall lines) suppresses O_3 concentration. As an overall effect, BVOC emissions have undermined or offset the progress achieved through anthropogenic emission controls, leading to only marginal reductions or, in some cases, even increases in O_3 concentrations (Fig. 5E).

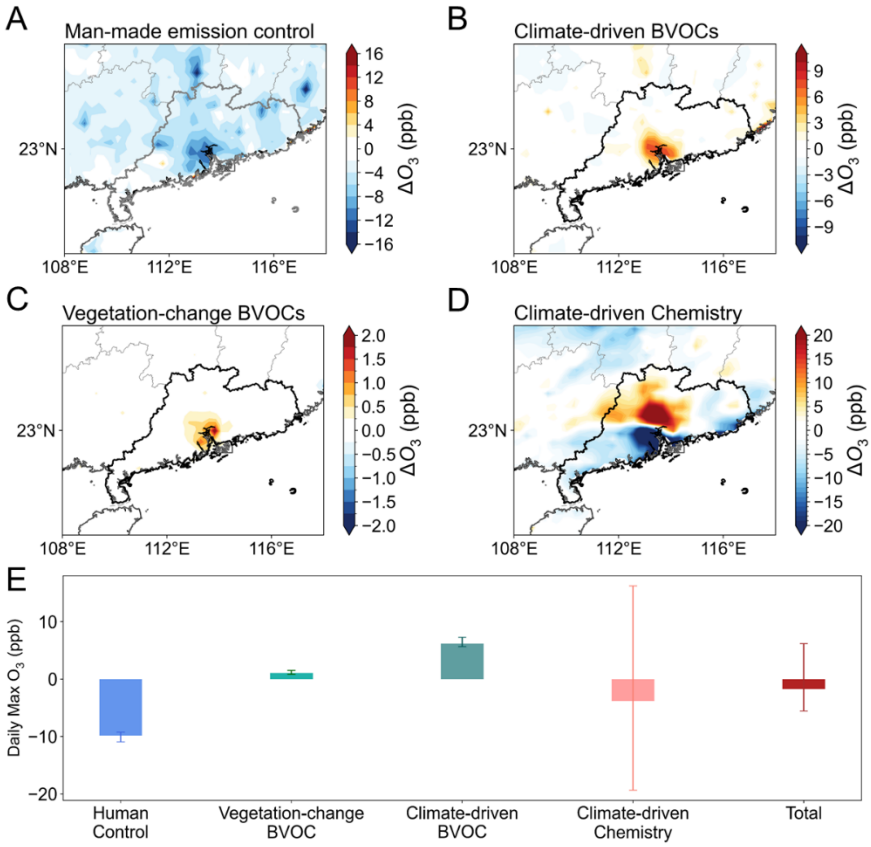

Figure 5. Impact of O_3 formation based on a maximal account for the influence of (A) man-made emission control, (B) climate-driven BVOC emissions, (C) vegetation-change BVOC, and (D) climate-driven meteorology on chemistry in the PRD region. (E) Daily max O_3 budget in Guangzhou city.

4. Conclusion and Implication

Due to the influence of the summer monsoon, O_3 concentrations in the PRD during summer are typically low and often overlooked. However, observational data indicates a rising trend in summer O_3 levels over the past decades, with an increase of approximately 1 ppb per summer. Based on the current understanding of O_3 formation sensitivity, it is widely acknowledged that the O_3 formation regime in the PRD tends to exhibit either a transitional or NOx-limited regime during summer. (Jin and Holloway, 2015; Wang et al., 2019). China's emphasis on reducing nitrogen oxide emissions over the past decade is expected to have contributed to lower summer O_3 levels. In response to the unexpected rise in summer O_3, our dynamically calculated natural emissions reveal a significant increase in BVOC emissions in the region between 2001 and 2020. This increase was primarily driven by climate change and changes in vegetation cover,

with climate-driven BVOC emissions accounting for approximately 80% of the rise. The concurrent increase in atmospheric and soil temperatures emerged as the key factors driving this increase in BVOC emissions. Based on parallel numerical simulations using the WRF-CMAQ models, we found that vegetation emissions driven by climate warming have mitigated, and in some cases even offset, the effects of anthropogenic emission reductions, serving as a key factor in the unexpected rise of O_3 levels in the PRD (Fig. 6).

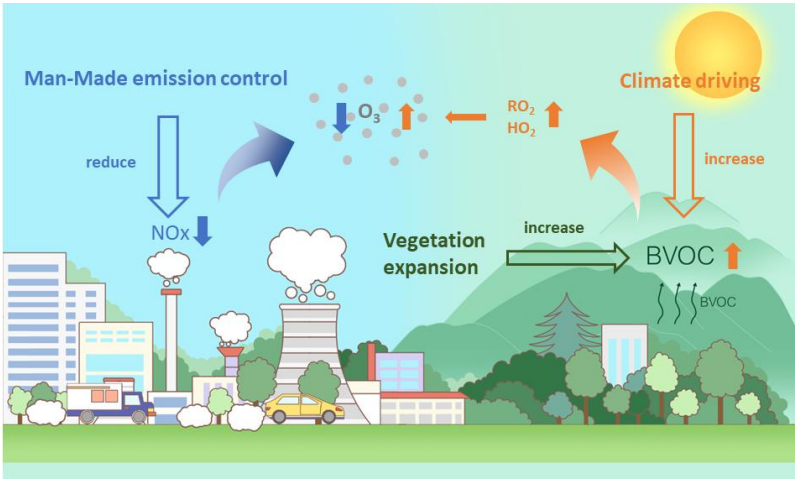

Figure 6. The conceptual scheme illustrating how climate-driven BVOCs emissions alleviate or offset man-made emission control against O_3.

China has proposed its ambitious strategies for carbon peaking and carbon neutrality, and for sure, will continue to enhance its efforts to reduce anthropogenic emissions. In the context of global warming, rising temperatures and carbon neutrality–induced greening are likely to enhance biogenic emissions, underscoring the increasing importance of natural sources in urban areas. Our findings highlight the significant role of climate-induced natural sources in tropospheric O_3 formation, even in regions with high anthropogenic activity, and emphasize the importance of mitigating climate warming. Lastly, it is recommended that future pollution control strategies shall take into account the synergistic effects of both anthropogenic and natural sources.

Acknowledgments

This research is supported by the National Key Research and Development Program (grant no. 2023YFC3709304), the National Natural Science Foundation Major Project (grant no. 42293322), the Youth Fund Project of the Sichuan Provincial Natural Science Foundation (24NSFSC2988), the special found of State Environmental Protection Key Laboratory of Formation and Prevention of Urban Air Pollution Complex (SEPAir-2024080211), the Guangdong Basic and Applied Basic Research Foundation (Grant No. 2022A1515011753), the Fundamental Research Funds for the Central Universities (Grant No. YJ202313) and Guangxi Science and Technology Program under Grant (No.AB24010074). The authors also thank the Tsinghua University for developing and sharing the MEIC emission inventory.

Data Availability Statement

Air pollutant data was collected through dynamic web scraping from the Environmental Monitoring Station of China: https://air.cnemc.cn:18007/. The O_3 sounding data at Hong Kong could be downloaded from: https://woudc.org/data/explore.php. Meteorological data from ERA5 are available at: https://cds.climate.copernicus.eu/datasets. The MODIS land data is from: https://e4ftl01.cr.usgs.gov/MOTA/. The numerical simulation results were stored in Tianhe-2 supercomputer, and results could be acquired from Dr. Nan Wang (nan.wang@scu.edu.cn)

Author Contributions

N.W. and H.L. designed the research. N.W. conducted the simulation and wrote the manuscript. N.W., H.L., W.X., and S.L. contributed to the interpretation of the results. All the authors provided critical feedback and helped to improve the manuscript.

Competing Interests

The authors declare that they have no known competing financial interests or personal relationships that could have appeared to influence the work.

References

Bonan, G. B., Levis, S., Kergoat, L., and Oleson, K. W.: Landscapes as patches of plant functional types: An integrating concept for climate and ecosystem models, Global Biogeochemical Cycles, 16, 5-1-5-23, 2002.

Cao, H., Fu, T.-M., Zhang, L., Henze, D. K., Miller, C. C., Lerot, C., Abad, G. G., De Smedt, I., Zhang, Q., and van Roozendael, M.: Adjoint inversion of Chinese non-methane volatile organic compound emissions using space-based observations of formaldehyde and glyoxal, Atmospheric Chemistry and Physics, 18, 15017-15046, 2018.

Cao, J., Situ, S., Hao, Y., Xie, S., and Li, L.: Enhanced summertime ozone and SOA from biogenic volatile organic compound (BVOC) emissions due to vegetation biomass variability during 1981–2018 in China, Atmospheric Chemistry and Physics, 22, 2351-2364, 2022.

Feng, Z., Xu, Y., Kobayashi, K., Dai, L., Zhang, T., Agathokleous, E., Calatayud, V., Paoletti, E., Mukherjee, A., and Agrawal, M.: Ozone pollution threatens the production of major staple crops in East Asia, Nature Food, 3, 47-56, 2022.

Fry, J. L., Draper, D. C., Barsanti, K. C., Smith, J. N., Ortega, J., Winkler, P. M., Lawler, M. J., Brown, S. S., Edwards, P. M., and Cohen, R. C.: Secondary organic aerosol formation and organic nitrate yield from NO3 oxidation of biogenic hydrocarbons, Environmental science & technology, 48, 11944-11953, 2014.

Fu, Y. and Liao, H.: Simulation of the interannual variations of biogenic emissions of volatile organic compounds in China: Impacts on tropospheric ozone and secondary organic aerosol, Atmospheric Environment, 59, 170-185, 2012.

Gao, Y., Ma, M., Yan, F., Su, H., Wang, S., Liao, H., Zhao, B., Wang, X., Sun, Y., and Hopkins, J. R.: Impacts of biogenic emissions from urban landscapes on summer ozone and secondary organic aerosol formation in megacities, Science of the Total Environment, 814, 152654, 2022.

Guenther, A., Karl, T., Harley, P., Wiedinmyer, C., Palmer, P. I., and Geron, C.: Estimates of global terrestrial isoprene emissions using MEGAN (Model of Emissions of Gases and Aerosols from Nature), Atmospheric Chemistry and Physics, 6, 3181-3210, 2006.

Guenther, A., Jiang, X., Heald, C. L., Sakulyanontvittaya, T., Duhl, T. a., Emmons, L., and Wang, X.: The Model of Emissions of Gases and Aerosols from Nature version 2.1 (MEGAN2. 1): an extended and updated framework for modeling biogenic emissions, Geoscientific Model Development, 5, 1471-1492, 2012.

Guenther, A., Hewitt, C. N., Erickson, D., Fall, R., Geron, C., Graedel, T., Harley, P., Klinger, L., Lerdau, M., McKay, W. A., Pierce, T., Scholes, B., Steinbrecher, R., Tallamraju, R., Taylor, J., and Zimmerman, P.: A global model of natural volatile organic compound emissions, Journal of Geophysical Research: Atmospheres, 100, 8873-8892, 10.1029/94JD02950, 1995.

Huang, X., Ding, A., Gao, J., Zheng, B., Zhou, D., Qi, X., Tang, R., Wang, J., Ren, C., and Nie, W.: Enhanced secondary pollution offset reduction of primary emissions during COVID-19 lockdown in China, National Science Review, 8, nwaa137, 2021.

Itahashi, S., Hayami, H., and Uno, I.: Comprehensive study of emission source contributions for tropospheric ozone formation over East Asia, Journal of Geophysical Research: Atmospheres, 120, 331-358, 2015.

Jenkin, M. E. and Clemitshaw, K. C.: Ozone and other secondary photochemical pollutants: chemical processes governing their formation in the planetary boundary layer, Atmospheric Environment, 34, 2499-2527, 2000.

552 Jin, X. and Holloway, T.: Spatial and temporal variability of ozone sensitivity over China observed
553 from the Ozone Monitoring Instrument, Journal of Geophysical Research: Atmospheres, 120,
554 7229-7246, 2015.
555 Li, L. and Xie, S.: Historical variations of biogenic volatile organic compound emission inventories
556 in China, 1981–2003, Atmospheric environment, 95, 185-196, 2014.
557 Li, L., Chen, Y., and Xie, S.: Spatio-temporal variation of biogenic volatile organic compounds
558 emissions in China, Environmental pollution, 182, 157-168, 2013.
559 Li, L., Yang, W., Xie, S., and Wu, Y.: Estimations and uncertainty of biogenic volatile organic
560 compound emission inventory in China for 2008–2018, Science of the Total Environment, 733,
561 139301, 2020.
562 Li, M., Huang, X., Yan, D., Lai, S., Zhang, Z., Zhu, L., Lu, Y., Jiang, X., Wang, N., and Wang, T.: Coping
563 with the concurrent heatwaves and ozone extremes in China under a warming climate, Science
564 Bulletin, 2024.
565 Lippmann, M.: Health effects of ozone a critical review, Japca, 39, 672-695, 1989.
566 Lu, X., Hong, J., Zhang, L., Cooper, O. R., Schultz, M. G., Xu, X., Wang, T., Gao, M., Zhao, Y., and
567 Zhang, Y.: Severe surface ozone pollution in China: a global perspective, Environmental Science &
568 Technology Letters, 5, 487-494, 2018.
569 Lyu, X., Li, K., Guo, H., Morawska, L., Zhou, B., Zeren, Y., Jiang, F., Chen, C., Goldstein, A. H., and Xu,
570 X.: A synergistic ozone-climate control to address emerging ozone pollution challenges, One Earth,
571 6, 964-977, 2023.
572 Ma, M., Gao, Y., Wang, Y., Zhang, S., Leung, L. R., Liu, C., Wang, S., Zhao, B., Chang, X., and Su, H.:
573 Substantial ozone enhancement over the North China Plain from increased biogenic emissions
574 due to heat waves and land cover in summer 2017, Atmospheric Chemistry and Physics, 19, 12195-
575 12207, 2019.
576 Seco, R., Holst, T., Davie-Martin, C. L., Simin, T., Guenther, A., Pirk, N., Rinne, J., and Rinnan, R.:
577 Strong isoprene emission response to temperature in tundra vegetation, Proceedings of the
578 National Academy of Sciences, 119, e2118014119, 2022.
579 Simon, H., Baker, K. R., Akhtar, F., Napelenok, S. L., Possiel, N., Wells, B., and Timin, B.: A direct
580 sensitivity approach to predict hourly ozone resulting from compliance with the National Ambient
581 Air Quality Standard, Environmental science & technology, 47, 2304-2313, 2013.
582 Wang, H., Lu, X., Seco, R., Stavrakou, T., Karl, T., Jiang, X., Gu, L., and Guenther, A. B.: Modeling
583 isoprene emission response to drought and heatwaves within MEGAN using evapotranspiration
584 data and by coupling with the community land model, Journal of Advances in Modeling Earth
585 Systems, 14, e2022MS003174, 2022a.
586 Wang, H., Wu, Q., Guenther, A. B., Yang, X., Wang, L., Xiao, T., Li, J., Feng, J., Xu, Q., and Cheng, H.:
587 A long-term estimation of biogenic volatile organic compound (BVOC) emission in China from
588 2001–2016: the roles of land cover change and climate variability, Atmospheric Chemistry and
589 Physics, 21, 4825-4848, 2021a.
590 Wang, N., Huang, X., Xu, J., Wang, T., Tan, Z.-m., and Ding, A.: Typhoon-boosted biogenic emission
591 aggravates cross-regional ozone pollution in China, Science Advances, 8, eabl6166, 2022b.
592 Wang, N., Lyu, X., Deng, X., Huang, X., Jiang, F., and Ding, A.: Aggravating O3 pollution due to
593 NOx emission control in eastern China, Science of the Total Environment, 677, 732-744, 2019.
594 Wang, N., Wang, H., Huang, X., Chen, X., Zou, Y., Deng, T., Li, T., Lyu, X., and Yang, F.: Extreme
595 weather exacerbates ozone pollution in the Pearl River Delta, China: role of natural processes,

Atmospheric Chemistry and Physics, 24, 1559-1570, 2024a.
Wang, N., Du, Y., Chen, D., Meng, H., Chen, X., Zhou, L., Shi, G., Zhan, Y., Feng, M., and Li, W.: Spatial disparities of ozone pollution in the Sichuan Basin spurred by extreme, hot weather, Atmospheric Chemistry and Physics, 24, 3029-3042, 2024b.
Wang, N., Xu, J., Pei, C., Tang, R., Zhou, D., Chen, Y., Li, M., Deng, X., Deng, T., Huang, X., and Ding, A.: Air Quality During COVID-19 Lockdown in the Yangtze River Delta and the Pearl River Delta: Two Different Responsive Mechanisms to Emission Reductions in China, Environmental Science & Technology, 55, 5721-5730, 10.1021/acs.est.0c08383, 2021b.
Wang, P., Zhang, Y., Gong, H., Zhang, H., Guenther, A., Zeng, J., Wang, T., and Wang, X.: Updating biogenic volatile organic compound (BVOC) emissions with locally measured emission factors in south China and the effect on modeled ozone and secondary organic aerosol production, Journal of Geophysical Research: Atmospheres, 128, e2023JD039928, 2023a.
Wang, T., Xue, L., Brimblecombe, P., Lam, Y. F., Li, L., and Zhang, L.: Ozone pollution in China: A review of concentrations, meteorological influences, chemical precursors, and effects, Science of the Total Environment, 575, 1582-1596, 2017.
Wang, Y., Zhao, Y., Liu, Y., Jiang, Y., Zheng, B., Xing, J., Liu, Y., Wang, S., and Nielsen, C. P.: Sustained emission reductions have restrained the ozone pollution over China, Nature Geoscience, 16, 967-974, 2023b.
West, J. J., Fiore, A. M., Horowitz, L. W., and Mauzerall, D. L.: Global health benefits of mitigating ozone pollution with methane emission controls, Proceedings of the National Academy of Sciences, 103, 3988-3993, 2006.
Wu, K., Yang, X., Chen, D., Gu, S., Lu, Y., Jiang, Q., Wang, K., Ou, Y., Qian, Y., Shao, P., and Lu, S.: Estimation of biogenic VOC emissions and their corresponding impact on ozone and secondary organic aerosol formation in China, Atmospheric Research, 231, 104656, https://doi.org/10.1016/j.atmosres.2019.104656, 2020.
Xiao, Q., Geng, G., Xue, T., Liu, S., Cai, C., He, K., and Zhang, Q.: Tracking PM2. 5 and O3 pollution and the related health burden in China 2013–2020, Environmental science & technology, 56, 6922-6932, 2021.
Yin, C., Solmon, F., Deng, X., Zou, Y., Deng, T., Wang, N., Li, F., Mai, B., and Liu, L.: Geographical distribution of ozone seasonality over China, Science of The Total Environment, 689, 625-633, 2019.
Zhang, X., Huang, T., Zhang, L., Shen, Y., Zhao, Y., Gao, H., Mao, X., Jia, C., and Ma, J.: Three-North Shelter Forest Program contribution to long-term increasing trends of biogenic isoprene emissions in northern China, Atmos. Chem. Phys., 16, 6949-6960, 10.5194/acp-16-6949-2016, 2016.